

The Role of Kapok Fiber in Modifying the Strength and Thermal Properties of Cement and Silica Fume Mortars: An Experimental Approach

Hakan SARIKAYA, Gülşah SUSURLUK*, Levent BOSTANCI

Abstract: Utilization of natural fibers into cementitious mixtures is gaining attention for their recyclability, renewability, sustainable features and other environmental benefits. Among varied natural fibers, kapok fiber (KP), a kind of lightweight and renewable natural fiber deserves attention for its ability to improve the strength and thermal insulation features of sustainable mortars and application of KP fiber in cementitious mixtures is still very limited. This research examined the impact of KP fiber on the strength features, pore structure, thermal insulation performance, and microstructure of ordinary Portland cement (OPC) and silica fume (SF) mixtures. The results indicated that KP incorporation at a content of 1% by cement weight leads to insulation enhancement up to 19% with 9.50% flexural strength gain. A linear regression analysis was conducted between pore structure characteristics and the determined strength/conductivity values to reveal the impact of KP fibers in the cement matrix. KP fiber has considerable potential to play a role in structural cementitious material design as a sustainable material.

Keywords: kapok fiber (KP); mechanical strength; pore structure; silica fume; thermal insulation

1 INTRODUCTION

The construction industry relies on mostly cement-based materials, largely due to their versatility and the accelerating demands of global economic expansion and urbanization. It is a well-known fact that cementitious materials are among the most widespread construction supplies in this sector, especially owing to the rapid growth of the global economy and urbanization [1-5]. Although calcination of clay and limestone as fundamental raw materials is essential for cement production, the calcination process results in significant amount of carbon dioxide (CO₂) emissions. Although technologies to reduce CO₂ emissions have been developed in recent years, cement production alone is still responsible for 7% of worldwide CO₂ emissions [3, 6]. However, the available stock of clay and limestone in nature is also consumed day by day by the cement industry for clinker production. Current energy efficiency and sustainability policies encourage the utilization of manufacturing by-products as alternative options for conventional OPC owing to their sustainable features [3, 7-9]. By-products of industrial processes, including slag, silica fume and fly ash are frequently utilized as alternative binders, recognized for their diminished CO₂ emissions and lowered energy demands. [8, 10, 11]. Among other industrial by-products, SF from the smelting industry indicates a great potential to replace ordinary cement in the mortar matrix, providing a sustainable and eco-friendly beneficial alternative [3, 12]. Previous studies clearly reveal that SF enhances the strength features of cementitious materials via encouraging the consumption of calcium hydroxide (CH), which leads to the formation of additional strength-enhancing calcium silicate hydrate (C-S-H) bonds [13, 14]. In general, calcium hydroxide (CH) consumption during SF-incorporated cement hydration is generally due to the superior activation ability of SF in chemical reactions [3]. Moreover, SF particles are 100 times finer than ordinary cement particles, enabling positively the reaction kinetics and related mechanical properties.

In order to reduce the carbon footprint and enhance the environmental performance of cement-based mixtures, concurrently increasing their mechanical and insulating

properties has become significant in sustainable design [9, 15]. This necessitates the inclusion of many alternative sustainable materials into the production process of cementitious materials, including natural fibers and industrial products of manufacturing for a partial replacement of cement in the binder content such as SF [15]. When natural fibers with high mechanical features reinforce the matrix such as mortar or concrete, they deeply influence the strength properties of the reinforced matrix by restricting the development of initial cracks and enhancing both the strength and insulation performance of cement-based materials, especially against micro cracks. Hence, recently, the integration of kapok fiber, a natural renewable fiber, into cement-based mix designs has been increasingly investigated in line with sustainable design objectives [16]. Kapok fiber, a natural seed-based material similar to cotton, possesses a density that is approximately one-seventh of cotton's density [16, 17]. Kapok fiber, obtained from the seed pods of the kapok tree, has an annual global production of approximately 40000 to 50000 metric tons. Of this, nearly 10000 metric tons are employed in eco-friendly applications, including textiles and insulation materials. Major producers include Brazil, the Philippines, and Indonesia [16]. Additionally, kapok fiber possesses one of the highest buoyancies among natural fibers, with a void ratio of up to 90% [16, 17]. In cementitious materials, the incorporation of KP demonstrates superior mechanical performance and thermal properties comparable to other natural fibers, offering exceptional features such as thermal and sound insulation [16, 18]. Nevertheless, there is no research on its incorporation into industrial by-product incorporated mortar mixtures, and its performance in terms of accessibility has not been thoroughly investigated.

A review of the current literature indicates that insufficient focus has been directed towards the combined impact of utilizing SF and textile fibers in mortar mixture designs. Particularly, research conducted by Xin et al. [1], Nawab et al. [2], Ja'e et al. [15], Alharthai et al. [19], Buller et al. [20], Haigh [21], Wu et al. [22], Subharaj et al. [23], Chen et al. [24], Koksai et al. [25], Ahmad and Chen [26], Aydın and Baradan [27] has predominantly focused on the inclusion of SF and various fibers in concrete or mortar

mixtures, examining primarily the mechanical properties of these compositions. Currently, however, there is an absence of research specifically investigating the insulation performance of mortar mixtures that incorporate both SF and KP. Besides mechanical and thermal performance, microstructural development and the properties of the interfacial transition zones (ITZs) are significant for affecting the overall behavior of cement-based systems. Prior research has demonstrated that the incorporation of aggregates or fibers can markedly affect the ITZs structure, micro crack propagation, and ultrasonic wave transmission in high-strength concrete [28]. Classical research on the ITZs emphasized that microstructural variability surrounding aggregates influences strength and durability performance [29]. Furthermore, the inclusion of pozzolanic materials like silica fume has been reported to improve the interfacial transition zone through the formation of secondary C-S-H products, hence enhancing pore densification and matrix-fiber interaction. Considering this context, additional examination of pore structure and ITZs development is essential for assessing the impact of kapok fibers mixed with SF in sustainable mortar mixtures. This investigation employs MIP and SEM analysis to investigate pore evolution and microstructural morphology in OPC and SF-based mortars. This study is pioneering in the exploration of kapok fiber as an additive in mortar mixtures, especially in combination with a OPC-SF binder, which has not been previously investigated. By incorporating KP into both pure conventional OPC and SF-incorporated OPC mortar mixtures, this research aims to assess its impacts on mechanical properties, thermal conductivity, porosity and microstructural morphology. There are very few studies in the literature on the use of kapok fiber, a distinctive member of the natural fiber family, in cement-based composites. In this context, the investigation of the possible positive effects of kapok fiber, owing to its natural mechanical and thermal properties, on the flexural strength and thermal insulation performance of mortar specimens constitutes the main rationale of this study. The scope of the research is significant in that it evaluates both mechanical strength and thermal insulation properties together. In this regard, the study aims to present a new perspective on the potential use of not only kapok fiber but also other natural fibers in cement-based composites.

2 MATERIALS AND METHODS

2.1 Materials

2.1.1 Binders

This study utilized OPC and SF as binding materials. Afyon Cement Factory produced OPC 42.5 R. Besides OPC, SF with a specific gravity of 2.31 g/cm³, sourced from Elkem Microsilica, was utilized in the investigation. Tab. 1 displays the components of chemical and physical features for the utilized OPC and SF.

2.1.2 Sand and Water

Tap water was employed in the preparation of the mixes. RilemCembureau standard sand, sourced from Trakya Limak Cement Factory, was utilized as the

aggregate for the mortar mixes in compliance with TS EN 196-1 [30]. The sand exhibited a density of 1.33 kg/dm³ and a saturated surface-dry specific gravity of 2.65.

Table 1 The components of chemical and physical features of utilized OPC and SF

Components of chemical / wt/wt%	OPC	SF
SiO ₂	19.1	85
Al ₂ O ₃	5.19	0.48
Fe ₂ O ₃	2.65	1.27
CaO	63.4	1.00
MgO	1.83	0.32
SO ₃	2.95	2.00
K ₂ O	0.94	0.89
Na ₂ O	0.22	0.27
Cl ⁻	0.01	0.3
Physical features		
Density / g/cm ³	1.05	2.31
Specific surface area / cm ² /g	3860	3500

2.1.3 Kapok Fiber

Kapok fiber is a lightweight natural fiber with a density of 0.29, a length of 20-35 mm, a diameter of 15-20 μm, and a moisture content of 6-8%.

2.1.4 Mix Proportions

To examine the effect of incorporating KP on the strength features, thermal conductivity, pore structure, and microstructural morphology of mortar specimens, eight different mortar mixtures were prepared. In all the mixes, the total quantity of cementitious components was maintained constant, the 4 of the mortar mixtures were prepared with binder content of 100% OPC and in the remaining 4 mixtures OPC to SF ratio was fixed at 1:1, by weight. A consistent water-to-cement ratio of 0.5 was maintained across all eight mixes. The proportions of the mixture are provided in Tab. 2 and labeled with specific codes as KP-0, KP-0.5, KP-0.75, KP-1, KP/SF-0, KP/SF-0.5, KP/SF-0.75 and KP/SF-1.

- KP-0 and KP/SF-0: plain mortars, in which no KP fiber added.
- KP-0.5, KP-0.75, and KP-1: fiber-reinforced mortars prepared with only OPC as the binder material.
- KP/SF-0.5, KP/SF-0.75, KP/SF-1: fiber-reinforced mortars prepared with OPC and SF as binder materials.

The numbers followed by "0", "0.5", "0.75", and "1.0" represent the fiber content incorporated into the mortar mixture, expressed as a percentage of the total binder weights.

Table 2 The proportions of mortar mixtures

Mix	KP fiber / gr	OPC / gr	SF / gr	Sand / gr	Water / ml
KP-0	-	450	-	1350	225
KP-0.5	2.25	450	-	1350	225
KP-0.75	3.375	450	-	1350	225
KP-1	4.5	450	-	1350	225
KP/SF-0	-	225	225	1350	225
KP/SF-0.5	2.25	225	225	1350	225
KP/SF-0.75	3.375	225	225	1350	225
KP/SF-1	4.5	225	225	1350	225

2.1.5 Mortar Specimens Casting, Curing and Testing Methodologies

Each raw component above mentioned above was weighed in a precision scale and mixed in the Hobart mixer. After-mixing method (kapok fibers were added after the solid components) recommended by Gao et al. was implemented [31]. Initially, the solid raw components, such as Portland cement, SF and sand, were added together and mixed for a duration of 1 minute. Additionally, water was incrementally added to the dry mixture and mixed for one more minute, followed by a further 2 minutes mixing to achieve a uniform mortar matrix. Prior to the addition of fibers, it is important for the fresh mixture to achieve uniform properties and adequate workability. After confirming the absence of any clumps at the bottom of the mixer, KP fiber was carefully incorporated to prevent the creation of fiber clumping and well blended in order to ensure uniform fiber dispersion [32, 33].

Prismatic specimens measuring $40 \times 40 \times 160$ mm were cast in triplicate from the fresh mortar mixtures, following the guidelines specified in TS EN 196-1 [28]. The specimens were kept in molds for the initial 24 hours and maintained at a temperature of 21 ± 1 °C during this period. A mechanical vibration treatment was applied to specimens for homogenization. The specimens were demolded the following day and subjected to a 28-day water curing process before the testing period. Fig. 1 illustrates the process flow diagram for specimen preparation.

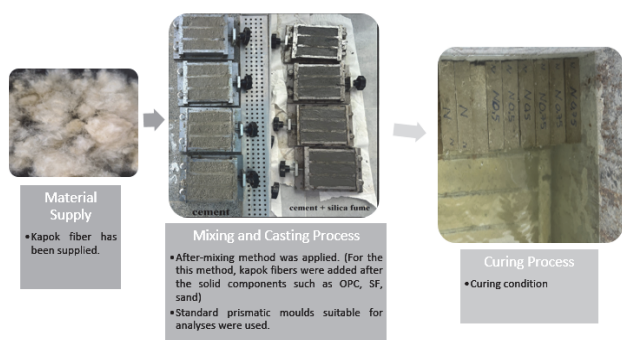


Figure 1 The process flow diagram for specimen preparation

Specimens subjected to a 28-day curing process were assessed to determine their flexural strength. The measurements for the three-point flexural test were performed in compliance with the standard TS EN 1015-11 [34]. To ensure reproducibility, strength tests were performed in triplicate, and the compressive strength values were calculated as the average of three fractured specimens obtained from flexural tests, with a contact surface of 40×40 mm, in compliance with the TS EN 1015-11 [34] standard. Fractured specimens from mechanical tests were further utilized for assessing thermal conductivity, pore structure characteristics, and microstructural features. Thermal conductivity measurements were performed at 21 ± 1 °C in accordance with ASTM D7984-16 [35], after oven-drying fractured specimens at 50 ± 5 °C for 24 h. Thermal conductivity of the mortar specimens was measured utilizing a TCI Thermal Conductivity Analyzer, with results expressed in

W/mK. Data were conducted a minimum of five times on various surfaces of each specimen, and the reported thermal conductivity values indicate the arithmetic mean of 5-8 individual measurements, depending on the consistency of the measurements.

The mercury intrusion porosimetry (MIP) was utilized to analyze the pore structure characteristics of the mortar specimens, including total porosity, pore size distribution, and critical pore content. The MIP measurements were conducted with a QTM-500 device, which can detect pore sizes from 3 to 360 micrometers. The surface morphological structures of the mortar specimens were analyzed using a LEO 1430 VP scanning electron microscope (SEM). Prior to the morphology analysis, the dry specimens were coated with a thin carbon layer. The relationship between pore structure features and the microstructural morphology of the reinforced matrix at fracture surfaces was examined.

3 RESULTLS AND DISCUSSIONS

3.1 Compressive Strength

The compressive strengths belonging to OPC and SF mortar specimens containing different amount of KP fiber at 28-day are presented in Fig. 2.

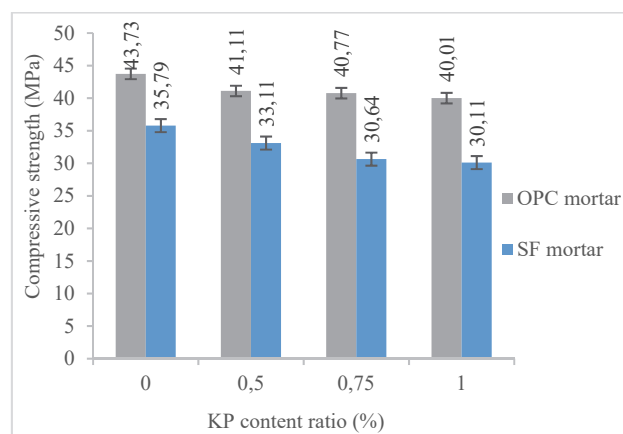


Figure 2 Compressive strengths test results of OPC and SF mortar specimens

The incorporation of fibers into a cement matrix is widely recognized to induce significant alterations in the matrix, impacting strength by increasing the total voids and restricting fracture propagation [36]. Fig. 2 illustrates that the incorporation of kapok fibers led to reduced compressive strengths in both OPC and SF mortars, although it is not significant in OPC mortars as it does not exceed 8.50% in comparison to KP-incorporated SF mortars. At 28 days of age, the OPC mortar specimen without the fibers achieved a compressive strength of 43.73 MPa. The inclusion of KP to the OPC mortar mixtures at ratios of 0.5%, 0.75%, and 1% resulted in reductions in compressive strength of 5.99%, 6.76%, and 8.50%, respectively. KP/SF-0 reached a compressive strength of 35.79 MPa with a curing period of 28 days. The incorporation of KP into the SF mortar mixes at content ratios of 0.5%, 0.75%, and 1% resulted in compressive strength decreases of 7.48%, 14.38%, and 15.87%, respectively. The analysis of OPC and SF mortar content groups revealed a consistent trend in compressive strength

following 28 days of curing: an increased incorporation content ratio of KP resulted in diminished compressive strength. This finding highlights a decrease with the increase in the fiber amount emphasizing the necessity of adjusting fiber content to minimize reductions in compressive strength and achieving an expected compressive strength target [37-41].

Furthermore, the inclusion of KP fibers in the mortar mixes caused a lower decrease in compressive strength for the OPC mortar content groups comparable with the SF mortar content groups. The observed effect has been emphasized to be related to the redistribution of the void structure caused by the inclusion of fibers, as well as the existence of inadequate interfacial adhesion between the fibers and the cement-SF grains [42]. However, it can reasonably be assumed that there were no dramatic reductions for compressive strength of specimens containing KP.

3.2 Flexural Strength

Enhanced flexural performance is one of the main advantages of fiber inclusion into cementitious mixtures as in the case of fiber existence additional energy is required for crack propagation and dissociating the connection between matrix and fiber [43]. In comparison to widely used man-made fibers such as carbon fiber, polypropylene, polyethylene etc, natural fibers are receiving attention for their economic and environmentally sustainable properties, offering them powerful alternatives to synthetic fibers [44]. Previous studies reported that most of natural fibers deeply improve the flexural performance of reinforced matrix such as were, respectively, 38%, 33%, 13% and 14% flexural strength enhancements in the case of agave lechuguilla fiber, flax fiber, hemp fiber, pig hair fiber incorporation into cementitious mixtures up to 1%, by weight [45]. Nevertheless, a substantial degree of effort remains necessary to evaluate the flexural performance of cementitious mixtures supplemented with natural fibers, such as kapok fiber, which are rarely used but have a good potential.

Flexural strengths of OPC and SF mortar specimens containing 0-1% KP fiber at 28-day are displayed in Fig. 3.

The 28-day flexural strengths of OPC and SF mortar mixture specimens containing KP were compared with the 28-day flexural strength of OPC and SF mortar mixture specimens without KP. The flexural strength values of the KP-0 and KP/SF-0 mortars prepared for comparison purpose were 11.58 and 8.11 MPa at 28 days, respectively. When compared to plain OPC mortar, the presence of KP fiber in OPC mortar increased the flexural strength by 2.59%, 4.92% and 8.63% for 0.5%, 0.75% and 1% fiber content proportions, respectively. In comparison to KP/SF-0 mortar, the presence of KP fiber in SF mortar increases the average flexural strength by 0.49%, 5.42% and 9.49% for 0.5%, 0.75% and 1% fiber content ratios, respectively. According to the findings, the analysis of OPC and SF mortar groups reveals that the rate of increase in flexural strength depends upon the amount of fiber. It is evident that even at 0.5% fiber content ratio, the incorporation of KP into OPC and SF mortar mixtures led to limited flexural strength enhancements but appreciable improvement in flexural strength is achieved regarding

fiber incorporation at a minimum amount of 0.75%. This finding demonstrates the significant impact of fiber content ratio on the flexural strength of mortar [37, 39-41,46-48]. Moreover, the inclusion of KP fibers in the mortar mixtures resulted in a more significant enhancement of flexural strength values for the SF mortar content groups in comparison to the OPC mortar content groups. This investigation revealed that the observed enhancement in the contribution of fibers to the flexural strength of mortar, in relation to mineral additives (such as SF), correlates with existing literature [49].

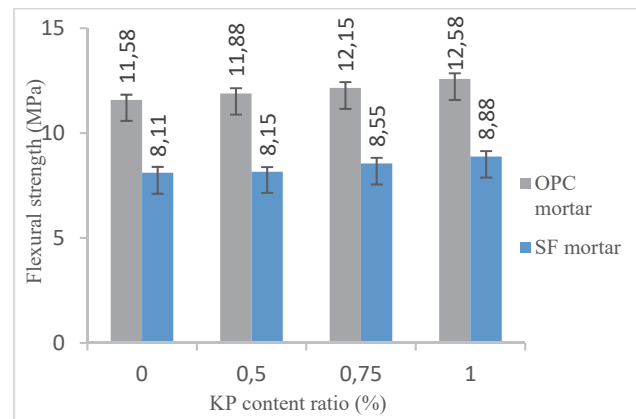


Figure 3 Flexural strength test results of OPC and SF mortar specimens

3.3 Thermal Conductivity

In the field of construction, there is an ongoing effort to lower energy consumption. This can be achieved via the use of insulation materials, which are designed to decrease heat loss and thermal conductivity. Besides, effective recycling of industrial, agricultural, and household waste is crucial in addressing environmental concerns [50]. At this point, the utilization of locally available and cheap natural fibers in cement-based mixtures appears to be a cost-effective and sustainable alternative, thereby transforming conventional cementitious materials into a compelling option for the design of new construction materials that prioritize energy efficiency and enhanced insulation properties [51]. With this in mind, Fig. 4 depicts the thermal conductivity of OPC and SF mortars for the incorporation content KP fiber up to 1%.

The thermal conductivity coefficients of OPC mortar mixtures incorporating KP ranged from 1.01 to 1.2 W/mK. As depicted in Fig. 4, the plain OPC mortar specimen demonstrated a thermal conductivity of 1.2 W/mK after a 28-day curing period. Incorporation of KP at ratios of 0.5%, 0.75% and 1% resulted in reductions in thermal conductivity by 7.91%, 10.83% and 15.83%, respectively. On the other hand, the thermal conductivity coefficients of SF mortar mixtures incorporating KP ranged from 1.05 W/mK. In comparison to control specimen with a thermal conductivity of 1.05 W/mK, decreases in thermal conductivity coefficients were measured as 5.23%, 9.52% and 19.04% for KP content ratios of 0.5%, 0.75% and 1%, respectively. The findings demonstrated that the incorporation of KP into OPC and SF mortar mixtures, even at a minimum content, significantly improved their thermal insulation properties. Previous research has shown that the inclusion of fibers significantly reduces heat

transfer, with thermal conductivity decreasing progressively as the fiber content increases [40, 46, 52]. Furthermore, the thermal insulation values of SF mortar specimens were determined to be superior compared to that of the OPC mortar specimen. The presence of natural fibers mostly leads to an increase in total porosity and a decrease in the density, making the fiber reinforced cement-based material thermally insulated in comparison to not reinforced case depending on the target behavior of the new material in mechanical-conductivity aspect [51]. Thermal conductivity results highlight the potential of incorporating both SF component and low fiber content into cement-based mixtures to enhance insulation properties. Besides, it could be also said that the beneficial effect of KP incorporation was greater in insulation performance compared to flexural gain at every content ratio of KP both in OPC and SF mortars. At this point, further experimental investigations could be focused on the development of such thermally insulated cementitious materials by the incorporation of KP into cementitious mixtures in an effort to develop its thermal insulating property with a partial flexural strength gain.

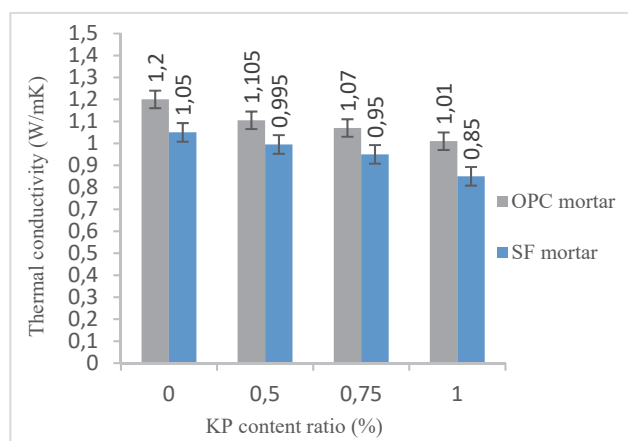


Figure 4 Measured thermal conductivity coefficients of OPC and SF mortar specimens

3.4 Mercury Intrusion Porosimetry (MIP)

The pore structure of cementitious materials plays an important role in detecting their mechanical performance and thermal insulation capabilities. The experimental mercury intrusion porosimetry (MIP) properties listed in Tab. 3 are important for evaluating the performance of these materials. Furthermore, it aligns with previous studies in the literature regarding the influence of pore structure on material properties and the role of fibers in enhancing these characteristics. For instance, incorporating fibers into cement-based materials has been shown to modify the pore structure, thereby improving overall material properties [3, 10, 16, 53]. Moreover, MIP is a commonly employed method for analyzing pore size distribution in cementitious materials [54]. Therefore, this research utilized MIP to examine the properties of pore structure characteristics of OPC and SF mortar specimens containing kapok fiber. The results, detailed in Tab. 3, provide valuable insights into how kapok fiber influences the pore structure parameters of these mortar specimens.

Table 3 MIP test results of mortar specimens

Mix	TP / %	TPA / m ² /g	MPDv / nm	MPDa / nm	APD (4V/A) / nm	BD / g/mL	AD / g/mL
KP-0	18.64	8.05	94.4	20.8	47.5	1.94	2.39
KP-0.5	21.65	8.60	106.7	21.1	54.3	1.85	2.36
KP-0.75	29.41	7.16	1131.4	25.2	95	1.72	2.44
KP-1	22.88	7.4	165.5	25	66.3	1.84	2.39
KP/SF-0	28.98	13.08	239.3	20.9	52.1	1.71	2.39
KP/SF-0.5	30.71	19.37	131.3	16.8	38.8	1.63	2.35
KP/SF-0.75	32.58	20.64	284.5	14.6	40.7	1.55	2.29
KP/SF-1	29.09	20.66	136.1	13.4	34.8	1.62	2.28

The MIP results presented in Tab. 3 demonstrate significant variations in the pore structure parameters of mortar specimens with different KP fiber content ratios and binder compositions. In general, the total porosity (TP) values increased with the addition of KP fibers in both the OPC and SF compositions. The highest TP was measured in the KP/SF-0.75 specimen, reaching 32.58%, which reflects the enhanced porosity associated with fiber-induced void formation. Incorporating fibers into the cement matrix can result in the development of voids around the fibers due to insufficient adhesion throughout the fibers and the matrix. This phenomenon has been observed in numerous studies, including those by Susurluk et al. [16] and He et al. [55]. The total pore area (TPA) exhibited a comparable trend particularly in the KP/SF compositions. In these compositions, TPA values were significantly higher compared to those in the OPC mortar specimens, highlighting the impact of the SF and kapok fiber combination on pore structure. The median pore diameter by volume (MPDv) exhibited significant increases with the incorporation of KP fibers, with the most significant increase observed in KP-0.75, where MPDv reached 1131.4 nm. This indicates that higher fiber content makes pores larger, likely due to poor adhesion and localized voids around the fibers. Conversely, the KP/SF compositions exhibited a more controlled increase in MPDv, suggesting that SF contributed to modifying the pore structure despite the presence of fibers. It is widely recognized that SF beneficially fills pores in cementitious matrix and this effect was observed at 0.75 and 1.0% KP contents in KP/SF mixes compared to OPC mortar mixes [56]. Furthermore, median pore diameter by area (MPDa) data may provide preliminary insight into the influence of the filling effect of SF on the cementitious pore system. MPDa values exhibited a continuous rise for the OPC mortar specimens corresponding directly to the KP fiber content ratio, whereas they demonstrated a continuous decrease for the SF mortar specimens. The reason for this increase may be the formation of less gaps with larger surface area diameters by fiber incorporation, considering the estimation of relatively higher total porosity values for all KP/SF compositions in comparison with KP/SF-0.

The average pore diameter (APD) and bulk density (BD) demonstrated notable variations, influenced by both fiber content and binder composition. For all mixtures, the bulk density (BD) exhibited a decreasing trend with increasing in KP fiber content, which can be ascribed to the formation of a porous matrix caused via the fibers, as expected. In line with this, the apparent density (AD) displayed a relatively decreasing trend compared to fiber

free cases, also indicating the porous modification of cementitious matrix caused by fiber addition. On the other hand, APD values displayed an overall rise with the inclusion of KP fibers in OPC mixtures. However, these values were consistently lower in the KP/SF specimens compared to the OPC mortar specimens, indicating the major pore filling effect of SF especially in higher fiber inclusion cases. Utilizing the SF into cementitious matrix lowered the measured APD values two times compared to OPC mixes which means SF indicates a great potential to decrease the detrimental effects of a high amount fiber in mixtures especially at fiber- matrix zone such as bond formation mechanism.

In order to investigate the strength changes against fiber incorporation, the role of the pore size distribution is compulsory to examine, as the type of distribution demonstrates the frequency of pores in regard to their size [57]. Fig. 5 demonstrates how KP fiber utilization impacts the pore system of OPC and SF mortar specimens, aged during 28 days. It is undoubted that the pore system in cementitious materials is very complicated [58]. Fig. 5a reveals the cumulative pore volume curves of OPC and SF mortar specimens at different amount of fiber inclusion cases. The cumulative pore intrusion curves of specimens incorporating KP are provided as preliminary source differing from tabulated MIP characteristics to give advanced pore system evaluation keynotes from other points of view. The peak intensities in the pore size distribution correspond with the detected total porosity values of the mortar specimens KP-0 (18.64%), KP-0.5 (21.65%) and KP-1 (22.88%), these specimens having the minimum values from bottom to top. Therefore, one can see that the curves for KP/SF-0.75 (32.58%) and KP/SF-0.5 (30.71%) are evidently higher than others. As known, the lower total specific pore volume can contribute to finer pore structure and intrusion curves are obviously influenced by the content of fiber [59]. Fig. 5b displays the relationship between the log-differential pore volume and specific pore-size ranges. SF-containing mixtures exhibit comparatively smoother trends, whereas increasing KP content results in more variation over a wider pore range. These observations indicate that both components influence the pore system characteristics of the mortar. In order to examine the effect of KP incorporation on various pore diameters, the pore system of mortar was divided into multiple pore ranges as 3-10, 10-100, 100-1000, 1000-10000, 10000-360,000, shown in Fig. 5c.

As indicated in Fig. 5c, the inclusion of KP fiber into the OPC mortar mixtures led to a higher proportion of pores within the size range of 1,000-360,000 nm. However, the incorporation of KP fiber into the OPC mortar mixtures caused a decline in pore sizes within the ranges of 3-10, 10-100 and 100-1,000 nm, in a general tendency. At this point, the decrease in the volume of gel pores (less than 10 nm) caused by fiber addition compared to fiber-free case clearly reveals the limited reductions detected in compressive strength values due to the major effect of gel pores on compressive strength gain [60]. It is obvious that the presence of KP fiber significantly dominated the pore system of the specimens, including the transformation of gel pore volume content to the large capillary and macro pores. The increases in the volume of capillary and macro pores are typically harmful to the mechanical performance

of the mortar; the pore size distribution highlights the strength loss [61].

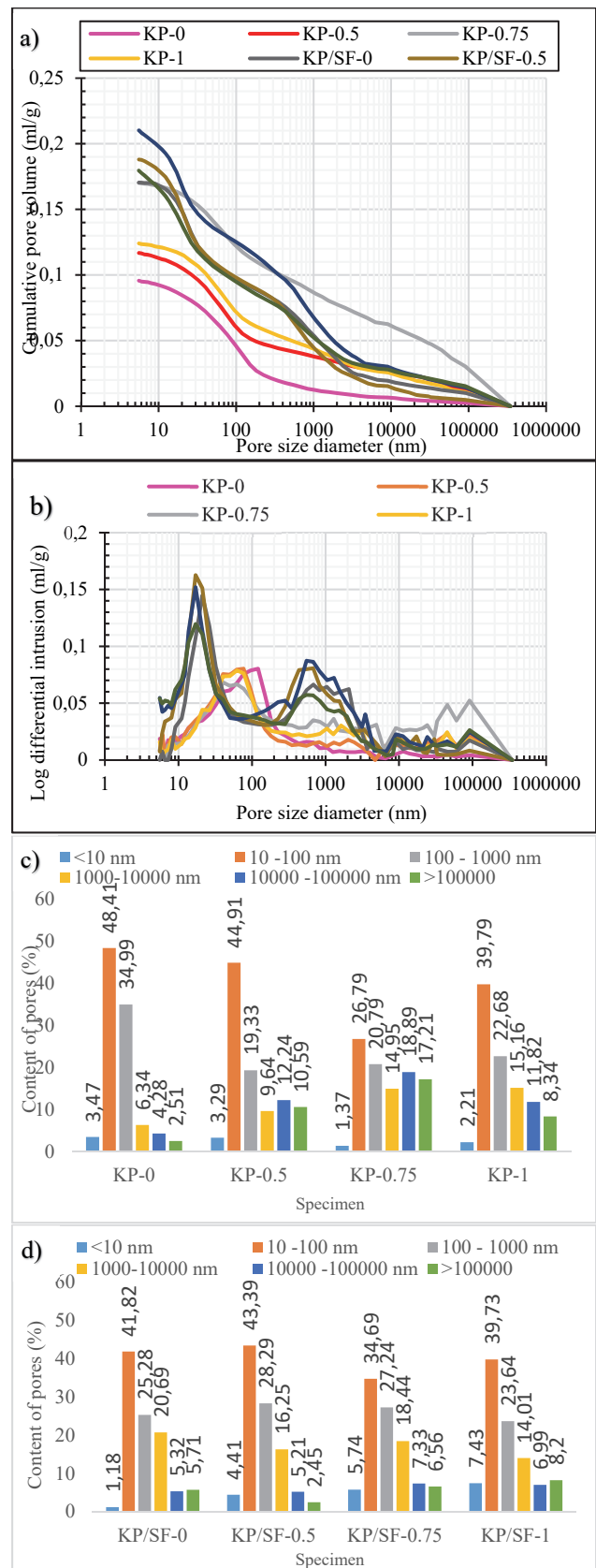


Figure 5 Effect of KP fiber addition on the pore system of OPC and SF mortar specimens

Fig. 5d depicts the volume of pores in abovementioned pore size ranges in silica fume mortar specimens. As indicated in Fig. 5c, while the minimum gel pore volume

(3-10 nm) formation identified in SF mortar specimen KP/SF-0 was 1.18%, higher pore contents in SF mortar specimens KP/SF-.5, KP/SF-0.75 and KP/SF-1 (4.41%, 5.74%, and 7.43%, respectively) were measured. This implies that the incorporation of KP fiber into the SF mortar mixtures triggered a chain of pore modification effective on gel pores due to the pore-filling effect of SF. On the other hand, the incorporation of KP fiber into the SF mortar mixtures led to a reduction in pore sizes within the ranges of 10-100, 100-1000, and 1000-10000 nm, in general. It is obvious that the presence of KP fiber considerably impacted the pore structure evolution of the specimens, notably influenced the volume of gel and macro pores. Öz et al. [62], Pi et al. [63], Sharma and Bishnoi [64] observed that increasing the fiber content in cement-based materials results in the development of pores, primarily attributed to the loosening of the interfacial transition zones (ITZs).

3.5 Relationship between Mechanical Performance, Pore Structure and Insulation

This investigation aims to improve the understanding of the impact of KP fiber utilization in OPC and SF mortar mixtures. In this work, linear regression analysis was carried out between pore structure features and determined strength/conductivity values in order to reveal if a relationship existed.

As illustrated in Fig. 6, strong linear correlations among compressive strength, flexural strength, pore structure, and thermal conductivity were discussed. Fig. 6a plots the compressive strength against the 1000-10000 pore volume fraction in KP-incorporated OPC mortars measured in this study. It is clearly seen that the increase in large capillary pores results in a limited decrease in compressive strength with a coefficient of correlation, $R^2 = 0.81$. This reduction is likely due to the stress concentration effect associated with larger pores, which act as weak points under load. In contrast, flexural strength demonstrated a positive linear correlation with pore content in the same size range (Fig. 6b), as indicated by an R^2 value of 0.84. The enhancement in flexural strength is due to the importance of KP fibers in reducing the spreading of fractures by bridging micro-cracks, especially within larger capillary pores. Additionally, the correlation between thermal conductivity and pore content in the size range of 1000-10000 nm (Fig. 6c) revealed an R^2 value of 0.87, indicating a substantial reduction in thermal conductivity with increasing pore content. This decrease is due to the insulating properties of air-filled capillary pores, which restrict heat transport networks inside the matrix.

The results presented in Fig. 7 demonstrate the experimental R^2 values derived from the relationships between pore structure development, thermal conductivity coefficient, and mechanical characteristics reveal the process of insulation - strength mechanism in kapok inclusion case. While the presence of larger capillary pores negatively impacts compressive strength, the same volume pores contribute positively to flexural strength and thermal conductivity. These findings underscore the critical role of pore development in enhancing the insulation and mechanical properties of cement-based materials [65-67].

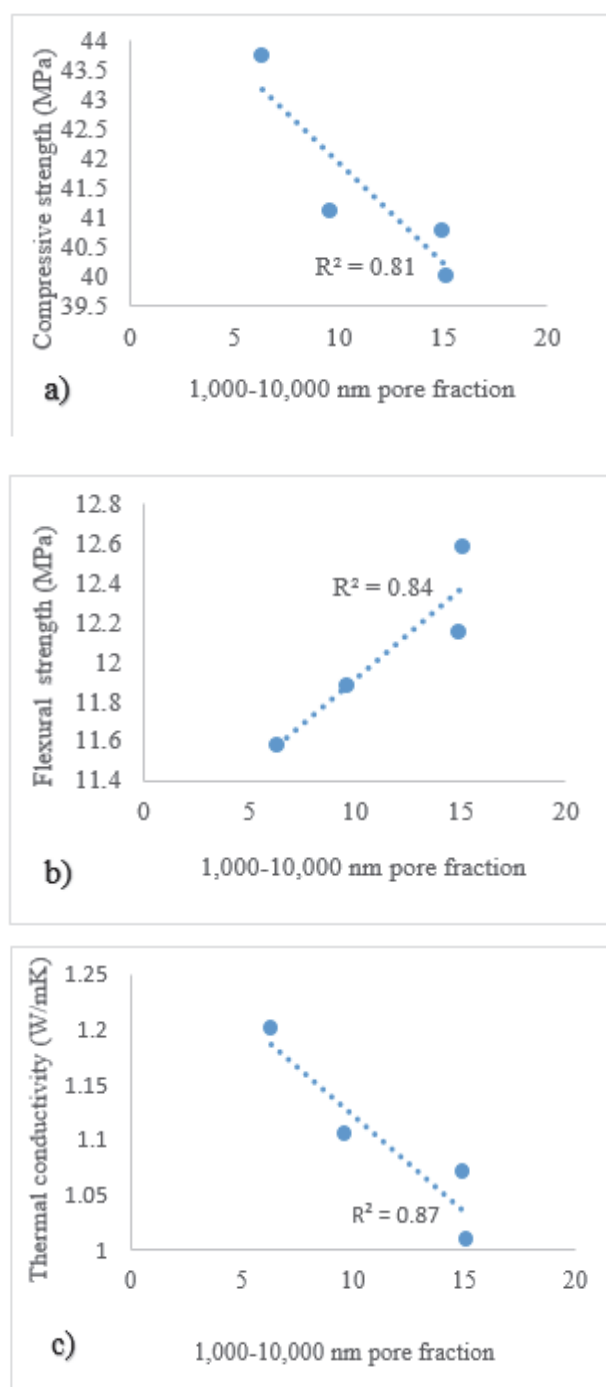


Figure 6 The correlation between the detected specific pore content - strengths/thermal conductivity in OPC mortars

As depicted in Fig. 7 strong linear correlations were also observed between pore content and the determined properties of KP fiber-incorporated SF mortar specimens. Fig. 7a shows a strong negative correlation ($R^2 = 0.96$) between compressive strength and pore content in the size range of < 10 nm. This indicates that as the proportion of gel pores increases, compressive strength decreases significantly. The gel pores, while beneficial for improving thermal performance, act as micro-voids that weaken the structural integrity of the mortar under compressive loads. In Fig. 7b, the correlation between compressive strength and larger capillary pores (10000-100000 nm) is weaker ($R^2 = 0.75$). These larger pores create localized stress concentrations, further reducing the material's capacity to withstand compressive forces. However, the lower R^2 value

suggests other factors, such as pore distribution and fiber-matrix bonding that may also contribute to strength variations. Fig. 7c demonstrates a positive linear relationship ($R^2 = 0.79$) between flexural strength and pore content in the < 10 nm range. This trend suggests that the formation of gel pores enhances the mortar's ductility by allowing stress redistribution, preventing brittle failure under flexural loads. The incorporation of KP fibers probably enhances this behavior by bridging micro-cracks and minimizing stress concentration effects. Fig. 7d shows a similar trend for flexural strength and pore content in the 10000-100000 nm range, with an R^2 of 0.76. The increase in flexural strength can be attributed to the structural reinforcement provided by KP fibers, which improve crack transmission resistance in the matrix, even in the presence of macro pores. Fig. 7e reveals a strong inverse relationship ($R^2 = 0.90$) between thermal conductivity and pore content in the < 10 nm range. The increase in gel pores is significantly leading to enhanced insulation properties. The high correlation highlights the role of SF in refining the pore structure, creating a dense matrix with improved thermal resistance. Fig. 7f shows a weaker correlation ($R^2 = 0.72$) between thermal conductivity and pore content in the 10000-100000 nm range. Macro pores also help reduce thermal conductivity by creating air voids in the matrix. However, their effect is less significant than gel pores because macro pores are irregularly distributed and vary in size. The incorporation of KP fibers in SF mortar specimens reveals unique variations in mechanical and thermal properties, as seen by the strong correlations in these figures. The formation of gel pores (< 10 nm) and macro pores (10000-100000 nm) significantly influences both compressive and flexural strength as well as thermal conductivity. These findings align with similar studies that emphasize the role of pore size distribution and fiber reinforcement in optimizing the performance of cement-based materials [68, 69].

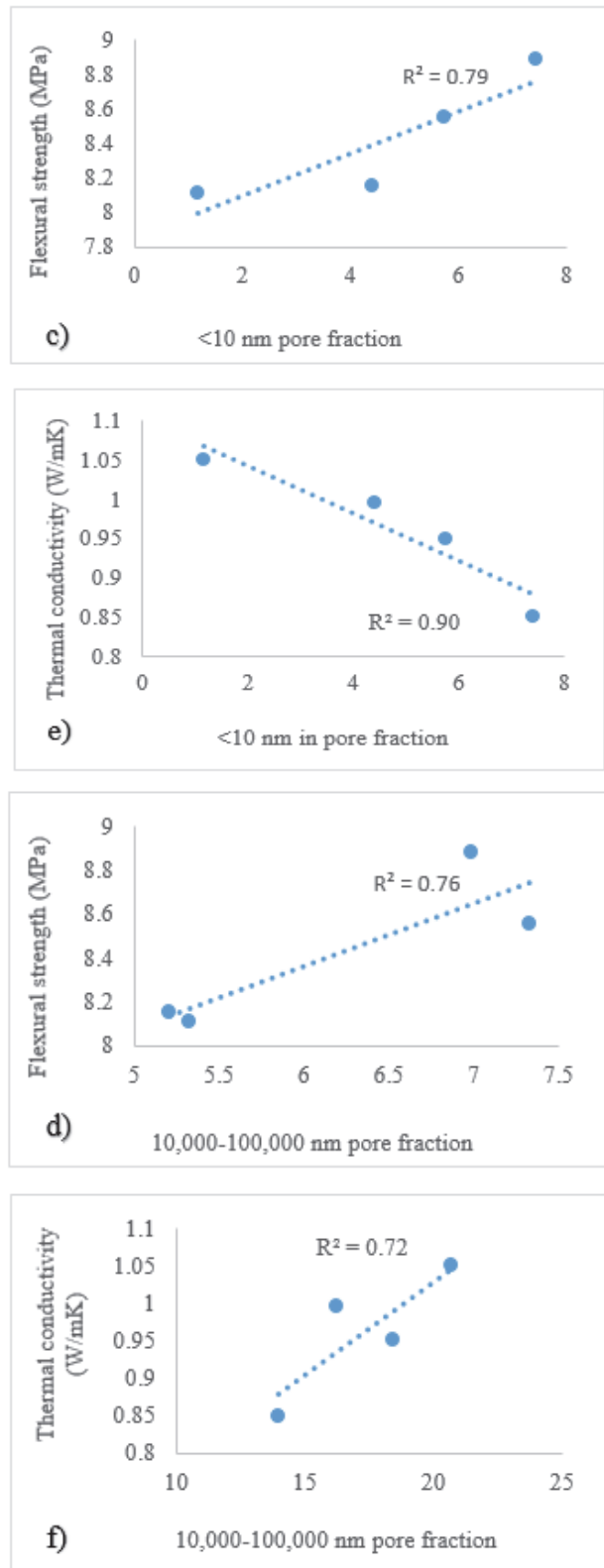
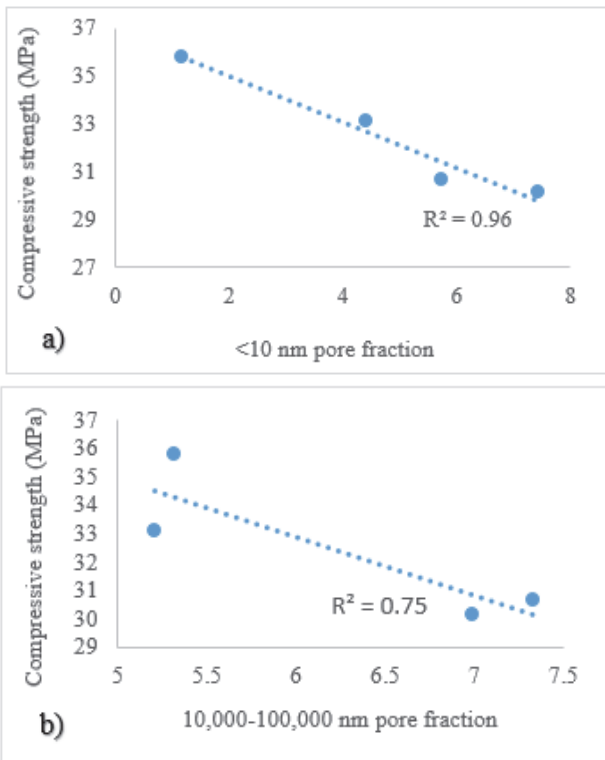


Figure 7 The correlation between the detected specific pore content- strengths/thermal conductivity in SF mortars

3.6 Scanning Electron Microscope (SEM) Analysis

Fig. 8 and Fig. 9 depict SEM images depicting the microstructural morphology of KP fiber-incorporated OPC and SF mortars, demonstrating how fiber content influences pore system and related morphology within the matrix. The SEM images highlight significant microstructural features, with yellow circles marking dense

matrix regions in fiber-free specimens, red circles indicating areas of C-S-H gel formation, and blue circles representing irregular porous zones and ettringite (Aft) transformations caused by fiber addition.

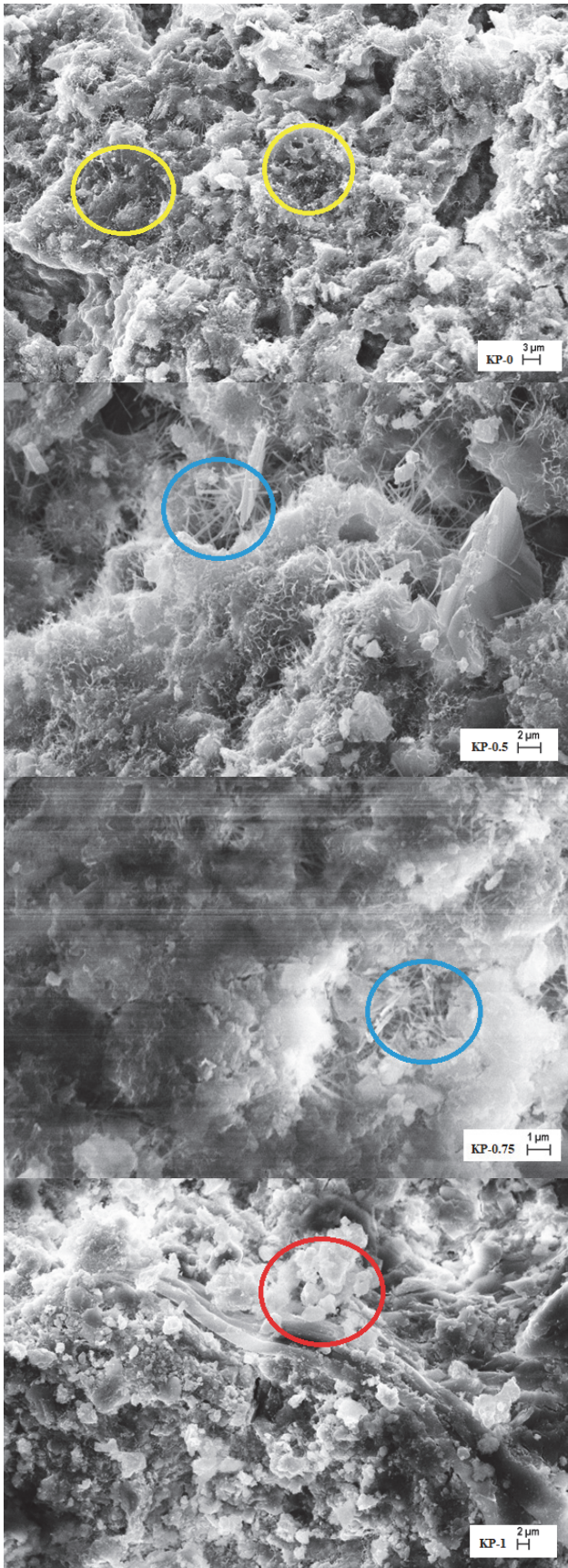


Figure 8 SEM micrograph demonstrating the microstructural morphology of KP fiber-incorporated OPC mortars

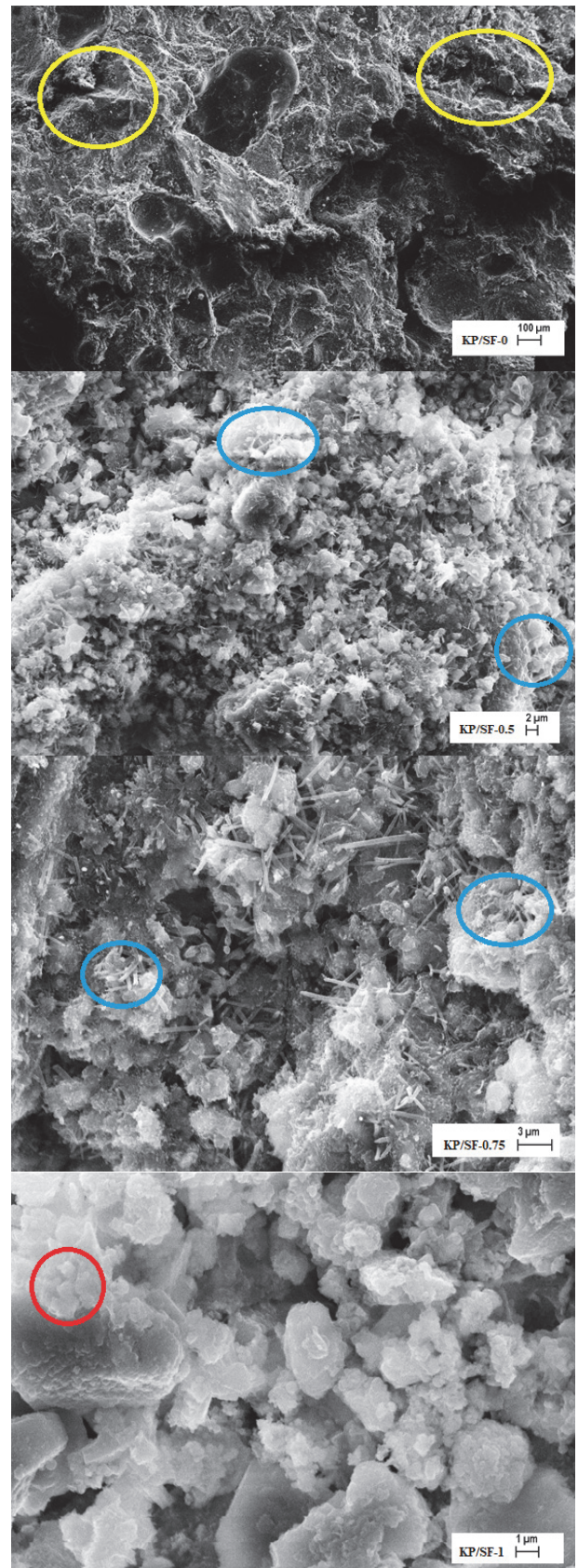


Figure 9 SEM micrograph demonstrating the microstructural morphology of KP fiber-incorporated SF mortars

To enhance comprehension of the hydration process in fiber-reinforced cement matrices, these observations must be taken into consideration with determined pore structure parameters. KP-0 and KP/SF-0 control mortar specimens displayed minimum total porosity values of 18.64% and

28.98%, respectively, in their own group. The pozzolanic reaction between $\text{Ca}(\text{OH})_2$ and SiO_2 produces C-S-H, which enhances the densification of the mortar and fills voids in the cementitious matrix, therefore decreasing pore [70]. Based on this effect, a more homogeneous and dense microstructure was observed in control specimens compared to fiber incorporated cases of their own group.

The incorporation of a little amount of KP fibers into the mortar mixtures caused an increase in the total porosity values for all specimens. However, changes in total porosity values seemed to be more sensitive to the fiber addition regardless of the flexural strength gain in OPC mortar specimens and in SF mortar specimens. This was largely attributed to the superior particle size, high specific surface area features and microscopic voids filling effect of the silica fume in the cementitious mix [70]. Moreover, while the total pore area decreased in OPC mortar specimens, it increased significantly in SF mortar specimens. The MIP analysis suggested that the maximum total porosity value was observed at a 0.75% content ratio in mixtures incorporating KP fibers in both OPC mortar and SF mortar. Accordingly, bubbles of air developed in KP-0.75 and KP/SF-0.75 mixes with the highest total porosity valued specimens, obviously observable in SEM micrographs.

The inclusion of fiber grains into the cement matrix is anticipated to increase the overall void formation, especially in the interfacial transition zones (ITZs) where fibers are incorporated, caused by potential weak adhesion. This phenomenon has been emphasized in research carried out via Susurluk et al. [16], Chu et al. [71], Li et al. [72]. Moreover, the addition of fibers within a cementitious matrix influences the microstructural development, particularly the formation of C-S-H gel [63, 73, 74]. C-S-H gel, as the primary hydration product, constitutes approximately 60-70% of the hydrated cementitious matrix and is crucial for mechanical strength development [75]. The SEM micrographs for OPC and SF mortar specimens with 1% KP fiber content ratio (KP-1 and KP/SF-1) highlight regions of C-S-H gel formation, marked in red circle. It is important to mention that KP-1 and KP/SF-1 specimens were found having the minimum total pore area and minimum average pore size detected specimens of their own fiber group and the development of a substantial quantity of C-S-H gels should be taken into consideration despite the maximum fiber content in the mixes. The microstructure of the OPC and SF mortars containing maximum fiber content appeared quite compact with uniform distribution of CSH hydration products. These observations also indicate that C-S-H gel formation plays a critical role in enhancing matrix bonding and contributing to the development of flexural strength. The enhancement in flexural strength is due to the reinforcement of the matrix by fibers, which effectively redistributes stress and bridges micro-cracks.

4 CONCLUSION

This study primarily investigated the incorporation of KP fiber into OPC and SF mortar mixtures. The findings allow for the following conclusions regarding the mechanical, thermal, pore structure, and microstructural properties:

- The results of the compressive strength test indicate that the inclusion of KP fiber led to a slight decline in compressive strength for both OPC and SF mortars. OPC mortars exhibited reductions between 5.99% and 8.50%, whereas SF mortars demonstrated higher declines, ranging from 7.48% to 15.87%, specifically related to enhanced porosity and in the matrix due to poor adhesion.
- The flexural strength test results demonstrate enhancement with the incorporation of KP fibers in both OPC and SF mortars. OPC mortars demonstrated enhancements ranging from 2.59% to 8.63%, whereas SF mortars displayed superior improvements of 0.49% to 9.49%, owing to the crack-bridging properties of the fibers.
- The results of the thermal conductivity test demonstrate that the incorporation of KP fibers substantially diminished thermal conductivity in both OPC and SF mortars. Reductions ranged from 7.91% to 15.83% in OPC mortars and from 5.23% to 19.04% in SF mortars, with the SF mortars showing superior insulation performance due to a more modified pore structure.
- The MIP test results revealed that KP fiber increased total porosity and influenced the distribution of pore sizes, particularly for SF mortar mixtures. The formation of both gel pores (< 10 nm) and capillary pores (10000-100000 nm) was more pronounced in SF mixtures, contributing to superior insulation performance.
- The SEM analysis confirmed that KP fibers influenced the interfacial transition zones and promoted the development for C-S-H bond, which improved flexural strength while maintaining acceptable compressive strength.

Despite the effort of utilizing the natural fibers into cementitious mortar mixtures in the literature, there is a deficiency in knowledge regarding the incorporation involving natural kapok fiber in sustainable mortar design. This experimental study approach is the first innovative design investigation of KP fiber in OPC and SF mortar mixtures. This investigation establishes kapok fiber as a promising natural fiber for sustainable mortar designs, particularly when combined with OPC and SF mixtures. The findings demonstrate an important understanding of the relationship among pore structure, mechanical performance, and thermal insulation in fiber-reinforced mortars. Future research could focus on advanced analytical methods, like X-ray computed tomography (CT) and 3D image analysis, to clarify the spatial distribution of pores and fibers, as well as their effects on mechanical and thermal properties. These preliminary insights will be remarkable to improving KP fiber-incorporated materials for sustainable construction applications.

As the next phase of this preliminary study, the performance of the multidimensional sustainable mortar under various durability conditions, together with a comprehensive Life Cycle Assessment (LCA) evaluating unit strength carbon emissions and unit service life, will further elucidate the sustainability advantages achieved through this approach.

5 REFERENCES

- [1] Xin, Q., Li, Z., Lu, S., Shao, P., & Zhang, M. (2024). The synergistic effect of recycled glass fiber reinforced plastic

- and silica fume on cement mortar properties. *Journal of Building Engineering*, 94, 110055. <https://doi.org/10.1016/j.jobe.2024.110055>
- [2] Nawab, M. S., Ali, T., Qureshi, M. Z., Zaid, O., Kahla, N. B., Sun, Y., Anwar, N., & Ajwad, A. (2023). A study on improving the performance of cement-based mortar with silica fume, metakaolin, and coconut fibers. *Case Studies in Construction Materials*, 19, e02480. <https://doi.org/10.1016/j.cscm.2023.e02480>
- [3] Bostanci, L. (2021). Effect of pore structure properties on strength properties of hybrid silica fume mortars containing randomly distributed carbon fibers. *Asian Journal of Civil Engineering*, 22, 1377-1399. <https://doi.org/10.1007/s42107-021-00389-6>
- [4] Liu, J., Tong, D., Zheng, Y., Cheng, J., Qin, X., Shi, Q., Yan, L., Lei, Y., & Zhang, Q. (2021). Carbon and air pollutant emissions from China's cement industry 1990-2015: Trends, evolution of technologies, and drivers. *Atmospheric Chemistry and Physics*, 21, 1627-1647. <https://doi.org/10.5194/acp-21-1627-2021>
- [5] Lu, B., Shi, C., Zhang, J., & Wang, J. (2018). Effects of carbonated hardened cement paste powder on hydration and microstructure of Portland cement. *Construction and Building Materials*, 186, 699-708. <https://doi.org/10.1016/j.conbuildmat.2018.07.176>
- [6] He, Z., Zhu, X., Wang, J., Mu, M., & Wang, Y. (2019). Comparison of CO₂ emissions from OPC and recycled cement production. *Construction and Building Materials*, 211, 965-973. <https://doi.org/10.1016/j.conbuildmat.2019.03.283>
- [7] Keeley, P. M., Rowson, N. A., Johnson, T. P., & Deegan, D. E. (2017). The effect of the extent of polymerisation of a slag structure on the strength of alkali-activated slag binders. *International Journal of Mineral Processing*, 164, 37-44. <https://doi.org/10.1016/j.minpro.2017.05.001>
- [8] Mehrabi, P., Shariati, M., Kabirifar, K., Jarrah, M., Rasekh, H., Trung, N. T., Shariati, A., & Jahandari, S. (2021). Effect of pumice powder and nano-clay on the strength and permeability of fiber-reinforced pervious concrete incorporating recycled concrete aggregate. *Construction and Building Materials*, 287, 122652. <https://doi.org/10.1016/j.conbuildmat.2021.122652>
- [9] Bostanci, L. (2022). Strength prediction of hybrid slag mortars containing chopped carbon fibers through pore features. *Iranian Journal of Science and Technology, Transactions of Civil Engineering*, 46, 4131-4150. <https://doi.org/10.1007/s40996-022-00918-6>
- [10] Bostanci, L. (2020). Effect of waste glass powder addition on properties of alkali-activated silica fume mortars. *Journal of Building Engineering*, 29, 101154. <https://doi.org/10.1016/j.jobe.2019.101154>
- [11] Chang, J. J. (2003). A study on the setting characteristics of sodium silicate-activated slag pastes. *Cement and Concrete Research*, 33, 1005-1011. [https://doi.org/10.1016/S0008-8846\(02\)01096-7](https://doi.org/10.1016/S0008-8846(02)01096-7)
- [12] Hu, C. & Li, Z. (2015). Property investigation of individual phases in cementitious composites containing silica fume and fly ash. *Cement and Concrete Composites*, 57, 17-26. <https://doi.org/10.1016/j.cemconcomp.2014.12.012>
- [13] Rossen, J. E., Lothenbach, B., & Scrivener, K. L. (2015). Composition of C-S-H in pastes with increasing levels of silica fume addition. *Cement and Concrete Research*, 75, 14-22. <https://doi.org/10.1016/j.cemconres.2015.04.016>
- [14] Xie, J., Zhang, Z., Lu, Z., & Sun, M. (2018). Coupling effects of silica fume and steel fiber on the compressive behavior of recycled aggregate concrete after exposure to elevated temperature. *Construction and Building Materials*, 184, 752-764. <https://doi.org/10.1016/j.conbuildmat.2018.07.040>
- [15] Ja'e, I. A., Sazrin, R., Syamsir, A., Bheel, N., Amaechi, C. V., Min, T. H., & Anggraini, V. (2024). Optimisation of mechanical properties and impact resistance of basalt fibre reinforced concrete containing silica fume: Experimental and response surface assessment. *Developments in the Built Environment*, 17, 100368. <https://doi.org/10.1016/j.dibe.2024.100368>
- [16] Susurluk, G., Sarikaya, H., & Bostanci, L. (2024). Utilization of natural kapok and coconut fiber in thermally insulated sustainable concrete design. *Environmental Science and Pollution Research*, 31, 61469-61490. <https://doi.org/10.1007/s11356-024-35324-0>
- [17] Damfeu, J. C., Meukam, P., & Jannot, Y. (2016). Modeling and measuring of the thermal properties of insulating vegetable fibers by the asymmetrical hot plate method and the radial flux method: Kapok, coconut, groundnut shell fiber, and rattan. *Thermochimica Acta*, 630, 64-77. <https://doi.org/10.1016/j.tca.2016.04.004>
- [18] Gobalakrishnan, M. & Saravanan, D. (2019). Thermal insulation properties of kapok/cotton blended non-woven fabric. *International Journal of Engineering and Advanced Technology*, 8.
- [19] Alharthai, M., Ali, T., Qureshi, M. Z., & Ahmed, H. (2024). The enhancement of engineering characteristics in recycled aggregates concrete combined effect of fly ash, silica fume and PP fiber. *Alexandria Engineering Journal*, 95, 363-375. <https://doi.org/10.1016/j.aej.2023.11.025>
- [20] Buller, A. S., Abro, F. R., Ali, M., Ali, T., & Bheel, N. (2024). Effect of silica fume on fracture analysis, durability performance, and embodied carbon of fiber-reinforced self-healed concrete. *Theoretical and Applied Fracture Mechanics*, 130, 104333. <https://doi.org/10.1016/j.tafmec.2024.104333>
- [21] Haigh, R. (2024). The mechanical behaviour of waste plastic milk bottle fibres with surface modification using silica fume to supplement 10% cement in concrete materials. *Construction and Building Materials*, 41, 135215. <https://doi.org/10.1016/j.conbuildmat.2024.135215>
- [22] Wu, R., Gu, Q., Gao, X., Luo, Y., Zhang, H., Tian, S., Ruan, Z., & Huang, J. (2024). Effect of basalt fibers and silica fume on the mechanical properties, stress-strain behavior, and durability of alkali-activated slag-fly ash concrete. *Construction and Building Materials*, 418, 135440. <https://doi.org/10.1016/j.conbuildmat.2024.135440>
- [23] Subharaj, C., Logesh, M., Munaf, A. A., Srinivas, J., & Gnanaraj, S. J. P. (2022). Sustainable approach on cement mortar incorporating silica fume, LLDPE and sisal fiber. *Materials Today: Proceedings*, 68, 1342-1348. <https://doi.org/10.1016/j.matpr.2022.04.111>
- [24] Chen, H., Wang, P., Pan, J., Lawi, A. S., & Zhu, Y. (2021). Effect of alkali-resistant glass fiber and silica fume on mechanical and shrinkage properties of cement-based mortars. *Construction and Building Materials*, 307, 125054. <https://doi.org/10.1016/j.conbuildmat.2021.125054>
- [25] Koksai, F., Yıldırım, M. S., Benli, A., & Gencil, O. (2021). Hybrid effect of micro-steel and basalt fibers on physico-mechanical properties and durability of mortars with silica fume. *Case Studies in Construction Materials*, 15, e00649. <https://doi.org/10.1016/j.cscm.2021.e00649>
- [26] Ahmad, M. R. & Chen, B. (2018). Effect of silica fume and basalt fiber on the mechanical properties and microstructure of magnesium phosphate cement (MPC) mortar. *Construction and Building Materials*, 190, 466-478. <https://doi.org/10.1016/j.conbuildmat.2018.09.114>
- [27] Aydın, S. & Baradan, B. (2013). The effect of fiber properties on high-performance alkali-activated slag/silica fume mortars. *Composites: Part B*, 45, 63-69. <https://doi.org/10.1016/j.compositesb.2012.05.022>
- [28] Hasannejad, M., Berenjian, J., Pouraminian, M., & Sadeghi Larijani, A. (2022). Studying of microstructure, interface transition zone and ultrasonic wave velocity of high-strength concrete by different aggregates. *Journal of Building Pathology and Rehabilitation*, 7(9).

- <https://doi.org/10.1007/s41024-021-00146-x>
- [29] Liao, K.-Y., Chang, P.-K., Peng, Y.-N., & Yang, C.-C. (2004). A study on characteristics of interfacial transition zone in concrete. *Cement and Concrete Research*, 34(6), 977-989. <https://doi.org/10.1016/j.cemconres.2003.10.020>
- [30] Turkish Standard Institute. (2009). *TS EN 196-1: Methods of testing cement: Part 1. Determination of strength*. Ankara, Turkey.
- [31] Gao, J., Wang, Z., Zhang, T., & Zhou, L. (2017). Dispersion of carbon fibers in cement-based composites with different mixing methods. *Construction and Building Materials*, 134, 220-227. <https://doi.org/10.1016/j.conbuildmat.2016.12.008>
- [32] Yang, E. H., Yang, Y., & Li, V. C. (2007). Use of high volumes of fly ash to improve ECC mechanical properties and material greenness. *ACI Materials Journal*, 104, 620-628. <https://doi.org/10.14359/18966>
- [33] Özbay, E., Karahan, O., Lachemi, M., Hossain, K. M. A., & Atis, C. D. (2013). Dual effectiveness of freezing-thawing and sulfate attack on high-volume slag-incorporated ECC. *Composites: Part B*, 45, 1384-1390. <https://doi.org/10.1016/j.compositesb.2012.07.046>
- [34] Turkish Standard Institute. (2000). *TS EN 1015-11: Methods of test for mortar for masonry: Part 11. Determination of flexural and compressive strength of hardened mortar*. Ankara, Turkey.
- [35] ASTM International. (2016). *ASTM D7984-16: Standard test method for measurement of thermal conductivity of polymer composites by means of a transient plane source (TPS) technique*. West Conshohocken, PA: ASTM International.
- [36] Shah, S. F. A., Chen, B., Oderji, S. Y., Haque, M. A., & Ahmad, M. R. (2020). Comparative study on the effect of fiber type and content on the performance of one-part alkali-activated mortar. *Construction and Building Materials*, 243, 118221. <https://doi.org/10.1016/j.conbuildmat.2020.118221>
- [37] Chen, Z., Zhao, G., Wei, J., Chen, C., & Tang, Y. (2024). Residual impact resistance behavior of PVA fiber reinforced cement mortar containing Nano-SiO₂ after exposure to chloride erosion. *Construction and Building Materials*, 414, 134990. <https://doi.org/10.1016/j.conbuildmat.2024.134990>
- [38] Dai, P., Lyu, Q., Zong, M., & Zhu, P. (2024). Effect of waste plastic fibers on the printability and mechanical properties of 3D-printed cement mortar. *Journal of Building Engineering*, 83, 108439. <https://doi.org/10.1016/j.job.2024.108439>
- [39] Lamichhane, N., Lamichhane, A., & Gyawali, T. R. (2024). Enhancing mechanical properties of mortar with short and thin banana fibers: A sustainable alternative to synthetic fibers. *Heliyon*, 10, e30652. <https://doi.org/10.1016/j.heliyon.2024.e30652>
- [40] Subashi De Silva, G. H. M. J., & Naveen, P. (2024). Effect of rice husk ash and coconut coir fiber on cement mortar: Enhancing sustainability and efficiency in buildings. *Construction and Building Materials*, 440, 137326. <https://doi.org/10.1016/j.conbuildmat.2024.137326>
- [41] Thapa, K., Sedai, S., Paudel, J., & Gyawali, T. R. (2024). Investigation on the potential of Eulaliopsisbinata (babiyo) as a sustainable fiber reinforcement for mortar and concrete. *Case Studies in Construction Materials*, 20, e03115. <https://doi.org/10.1016/j.cscm.2024.e03115>
- [42] Karahan, O. & Atis, C. D. (2011). The durability properties of polypropylene fiber reinforced fly ash concrete. *Materials and Design*, 32, 1044-1049. <https://doi.org/10.1016/j.matdes.2010.07.002>
- [43] Shu, X., Graham, R. K., Huang, B., & Burdette, E. G. (2015). Hybrid effects of carbon fibers on mechanical properties of Portland cement mortar. *Materials & Design*, 65, 1222-1230. <https://doi.org/10.1016/j.matdes.2014.10.033>
- [44] Han, Y., Shi, M., Lee, S., Lin, R., Wang, K. J., & Wang, X. Y. (2024). Application of porous luffa fiber as a natural internal curing material in high-strength mortar. *Construction and Building Materials*, 455, 139169. <https://doi.org/10.1016/j.conbuildmat.2024.139169>
- [45] Garcia, G., Cabrera, R., Rolón, J., Pichardo, R., & Thomas, C. (2024). Natural fibers as reinforcement of mortar and concrete: A systematic review from Central and South American regions. *Journal of Building Engineering*, 98, 111267. <https://doi.org/10.1016/j.job.2024.111267>
- [46] Evangelia, T., Ioanna, V., & Stefanidou, M. (2024). Effect of hemp fibers and crystalline admixtures on the properties and self-healing efficiency of lime and clay-based mortars. *Journal of Building Engineering*, 86, 108963. <https://doi.org/10.1016/j.job.2024.108963>
- [47] Yousef, S. & Kalpokaite-Dickuviene, R. (2024). Sustainable mortar reinforced with recycled glass fiber derived from pyrolysis of wind turbine blade waste. *Journal of Materials Research and Technology*, 31, 879-887. <https://doi.org/10.1016/j.jmrt.2024.06.134>
- [48] Zhang, M., Qiu, X., & Zhang, R. (2024). Enhancing alkali resistance of recycled GFRP fibers and mechanical performances of cement mortars with microbial induced carbonate precipitation. *Construction and Building Materials*, 438, 137091. <https://doi.org/10.1016/j.conbuildmat.2024.137091>
- [49] Xia, R., Zhang, N., Zhang, Y., Zhang, S., Wang, Y., Zhang, Y., & Zhou, Y. (2024). Effects of halloysite-decorated basalt fiber on mechanical properties and microstructure of iron tailings-based cementitious mortar. *Construction and Building Materials*, 417, 135300. <https://doi.org/10.1016/j.conbuildmat.2024.135300>
- [50] Benazzouk, A., Douzane, Q., Mezreb, K., Laidoudi, B., & Quéneudec, M. (2008). Thermal conductivity of cement composites containing rubber waste particles: Experimental study and modelling. *Construction and Building Materials*, 22(4), 573-579. <https://doi.org/10.1016/j.conbuildmat.2006.11.011>
- [51] Majumder, A., Stochino, F., Frattolillo, A., Valdés, M., Mancusi, G., & Martinelli, E. (2023). Jute fiber reinforced mortars: Mechanical response and thermal performance. *Journal of Building Engineering*, 66(3), 105888. <https://doi.org/10.1016/j.job.2023.105888>
- [52] Wang, Y., Li, L., Feng, X., Zheng, X., & Wu, Q. (2024). Sustainable utilization of fly ash for phase-change geopolymer mortar reinforced by fibers. *Construction and Building Materials*, 412, 134814. <https://doi.org/10.1016/j.conbuildmat.2023.134814>
- [53] Bostanci, L. (2020b). A comparative study of petroleum coke and silica aerogel inclusion on mechanical, pore structure, thermal conductivity and microstructure properties of hybrid mortars. *Journal of Building Engineering*, 31, 101478. <https://doi.org/10.1016/j.job.2020.101478>
- [54] Abell, A. B., Willis, K. L., & Lange, D. A. (1999). Mercury intrusion porosimetry and image analysis of cement-based materials. *Journal of Colloid and Interface Science*, 211(1), 39-44. <https://doi.org/10.1006/jcis.1998.5986>
- [55] He, J., Wang, X., Han, L., Wang, S., & Xin, M. (2024). Effect of graphene oxide on the electrothermal and pressure-sensitive properties of carbon fiber cementitious composites. *Materials*, 17(16), 3928. <https://doi.org/10.3390/ma17163928>
- [56] Huang, F., Liu, J., Li, X., Li, C., Hu, Z., Shen, X., & Chen, B. (2024). Impact of silica fume on the long-term stability of cement-based materials with low water-to-binder ratio under different curing conditions. *Construction and Building Materials*, 450, 138604. <https://doi.org/10.1016/j.conbuildmat.2024.138604>
- [57] Nguyen, T. B. T., Chatchawan, R., Saengsoy, W., Tangtermisirikul, S., & Sugiyama, T. (2019). Influences of different types of fly ash and confinement on performances

- of expansive mortars and concretes. *Construction and Building Materials*, 209, 176-186.
<https://doi.org/10.1016/j.conbuildmat.2019.03.032>
- [58] Wang, Y. S. & Dai, J. G. (2017). X-ray computed tomography for pore-related characterization and simulation of cement mortar matrix. *NDT & E International*, 86, 28-35.
<https://doi.org/10.1016/j.ndteint.2016.11.005>
- [59] Ying, J., Zhou, B., & Xiao, J. (2017). Pore structure and chloride diffusivity of recycled aggregate concrete with nano-SiO₂ and nano-TiO₂. *Construction and Building Materials*, 150, 49-55.
<https://doi.org/10.1016/j.conbuildmat.2017.05.168>
- [60] Nguyen, T. T., Bui, H. H., Ngo, T. D., Nguyen, G. D., Kreher, M. U., & Darve, F. (2024). A micromechanical investigation for the effects of pore size and its distribution on geopolymer foam concrete under uniaxial compression. *Engineering Fracture Mechanics*, 209, 228-244.
<https://doi.org/10.1016/j.engfracmech.2019.01.033>
- [61] Xuan, M., Geng, Y., & Sarkis, J. (2018). A review of sustainable product-service systems: State of the art and future trends. *Journal of Cleaner Production*, 187, 222-236.
<https://doi.org/10.1016/j.jclepro.2018.03.081>
- [62] Öz, A., Bayrak, B., Kaplan, G., & Aydın, A. C. (2023). Effect of waste colemanite and PVA fibers on GBFS-Metakaolin based high early strength geopolymer composites (HESGC): Mechanical, microstructure and carbon footprint characteristics. *Construction and Building Materials*, 377, 131064.
<https://doi.org/10.1016/j.conbuildmat.2023.131064>
- [63] Pi, Z., Xiao, P., Liu, R., & Liu, M. (2021). Quantitative analysis of steel fiber-matrix ITZ and multi-scale enhancement mechanism of SFRC. *Materials and Structures*, 54. <https://doi.org/10.1617/s11527-021-01825-4>
- [64] Sharma, M. & Bishnoi, S. (2018). The interfacial transition zone: Microstructure, properties, and its modification. *Recent Advances in Structural Engineering*, 2, 745-754.
https://doi.org/10.1007/978-981-13-0365-4_63
- [65] Sonar, K. & Sathe, S. (2024). Exploring fiber reinforcements in concrete and its challenges: A comprehensive review. *Multiscale and Multidisciplinary Modeling, Experiments and Design*, 7, 3099-3131.
<https://doi.org/10.1007/s41939-024-00404-8>
- [66] Li, L., Wang, W., Wang, Y., Li, D., & Zhuang, M. L. (2023). Experimental study on pore structure characteristics and thermal conductivity of fibers reinforced foamed concrete. *Plos One*, 18(7), e0287690.
<https://doi.org/10.1371/journal.pone.0287690>
- [67] Niu, D., Huang, D., Zheng, H., Su, L., Fu, Q., & Luo, D. (2019). Experimental study on mechanical properties and fractal dimension of pore structure of basalt-polypropylene fiber-reinforced concrete. *Applied Sciences*, 9(8), 1602.
<https://doi.org/10.3390/app9081602>
- [68] Khan, S. H., Rahman, M. Z., Haque, M. R., & Hoque, M. E. (2023). Characterization and comparative evaluation of structural, chemical, thermal, mechanical, and morphological properties of plant fibers. *Annual Plant: Sources of Fibres, Nanocellulose and Cellulosic Derivatives*, 1-45. https://doi.org/10.1007/978-981-99-2473-8_1
- [69] Ardanuy, M., Claramunt, J., Garcia-Hortal, J. A., & Barra, M. (2011). Fiber-matrix interactions in cement mortar composites reinforced with cellulosic fibers. *Cellulose*, 18, 281-289. <https://doi.org/10.1007/s10570-011-9493-3>
- [70] Rukzon, S., Rungruang, S., Chaisakulkiat, U., Posi, P., & Chindaprasirt, P. (2025). Strength, pore and corrosion characteristics of ceramic insulator powder-silica fume based ternary blended mortar. *Cleaner Materials*, 15, 100284. <https://doi.org/10.1016/j.clema.2024.100284>
- [71] Chu, S. H., Jiang, Y., & Kwan, A. K. H. (2019). Effect of rigid fibres on aggregate packing. *Construction and Building Materials*, 224, 326-335.
<https://doi.org/10.1016/j.conbuildmat.2019.07.072>
- [72] Li, H., Li, L., Li, L., Zhou, J., Mu, R., & Xu, M. (2022). Influence of fiber orientation on the microstructures of interfacial transition zones and pull-out behavior of steel fiber in cementitious composites. *Cement and Concrete Composites*, 128, 104459.
<https://doi.org/10.1016/j.cemconcomp.2022.104459>
- [73] Li, Z., Zhu, J., & Pei, C. (2024). Enhanced interfacial bonding in cement composites through electrophoretic deposition of nano silica on carbon fibers. *Construction and Building Materials*, 435, 136835.
<https://doi.org/10.1016/j.conbuildmat.2024.136835>
- [74] Lin, C., Kanstad, T., Jacobsen, S., & Ji, G. (2023). Bonding property between fiber and cementitious matrix: A critical review. *Construction and Building Materials*, 378, 131169.
<https://doi.org/10.1016/j.conbuildmat.2023.131169>
- [75] Scrivener, K. L. & Nonat, A. (2011). Hydration of cementitious materials, present and future. *Cement and Concrete Research*, 41(7), 651-665.
<https://doi.org/10.1016/j.cemconres.2011.03.026>

Hakan SARIKAYA

Construction Technology Programme, School of Advanced Vocational Studies,
 Usak University, Usak, Turkey
 E-mail: hakan.sarikaya@usak.edu.tr

Gülşah SUSURLUK

(Corresponding author)
 Textile Technology Programme, School of Advanced Vocational Studies,
 Istanbul Beykent University, Istanbul, Turkey
 E-mail: gulsahsusurluk@beykent.edu.tr

Levent BOSTANCI

Building Insulation Technologies Programme,
 School of Advanced Vocational Studies,
 Istanbul Beykent University, Istanbul, Turkey
 E-mail: leventbostanci@beykent.edu.tr